

STUDY OF GAS-SATURATED TURBULENT STREAMS
USING A LASER DOPPLER VELOCITY METER

Yu. N. Dubnishchev, A. R. Evseev,
V. S. Sobolev, and E. N. Utkin

UDC 532.526.4

New experimental results on the study of a turbulent gas-saturated stream in a tube using a laser Doppler velocity meter and a thermoanemometer are discussed. The distributions of the volumetric gas content over the cross section of the tube and profiles of the average velocities and average and pulsation characteristics of the shear stress at the wall in the stream under investigation are obtained. The experimental apparatus and the method of the measurements are described.

Gas saturation as a method of reducing hydrodynamic resistance has attracted the attention of investigators [1, 2]. The decrease in friction with gas saturation of the turbulent boundary layer is explained by a change in the physical constants of the gas-saturated liquid.

The dependence of the relative (apparent) viscosity of different liquids on the volumetric concentration of small gas bubbles is studied experimentally in [3, 4]. The results of the studies showed that the viscosity of a bubbly liquid is greater than the viscosity of a single-phase liquid. The relative increase in viscosity upon gas saturation of a liquid depends not only on the volumetric gas content, but also on the size of the gas bubbles.

In a theoretical study [5] the real bubbly medium is replaced by a certain homogeneous single-phase medium having physical constants which depend on the volumetric gas content. The results of the solution of the problem showed that the relative decrease in the hydrodynamic resistance upon gas saturation of the turbulent boundary layer is a function of a single parameter — the density of the gas-saturated liquid at the permeable wall.

A considerable change in the physical constants of a gas-saturated liquid must affect the properties of the boundary turbulence and the fine structure of the stream. The hypothesis that the gas bubbles can decrease the intensity of turbulent momentum exchange owing to the separation of adjacent layers of liquid in the boundary layer and through deformation of the bubbles was advanced in [6].

The experimental studies in the present work were performed on a hydrodynamic apparatus of gravitational operation.

The working section consisted of a horizontal tube with a rectangular cross section of 30×40 mm². A permeable layer 250 mm long was set in the bottom of the working section flush with it. The width of the permeable layer was less than the width of the working section (24 and 40 mm, respectively). The gas saturation of the turbulent stream in the tube was accomplished by blowing the gas through the permeable layer.

The permeable layer consisted of a set of closely pressed together sheets of plastic each 1 mm thick. Grooves were made by mechanical means on both sides of each sheet. Tests showed that owing to the grooves the slits between the closely pressed sheets represent a collection of pores with good uniformity of size. The pore sizes were determined from the separation diameter of the bubbles through a calculation by the equation of [7]. According to the estimates the mean pore size of the permeable layer was 2–4 μ . The surface porosity of the layer was ~1%.

Novosibirsk. Translated from *Zhurnal Prikladnoi Mekhaniki i Tekhnicheskoi Fiziki*, No. 1, pp. 147–153, January–February, 1975. Original article submitted February 15, 1974.

©1976 Plenum Publishing Corporation, 227 West 17th Street, New York, N.Y. 10011. No part of this publication may be reproduced, stored in a retrieval system, or transmitted, in any form or by any means, electronic, mechanical, photocopying, microfilming, recording or otherwise, without written permission of the publisher. A copy of this article is available from the publisher for \$15.00.

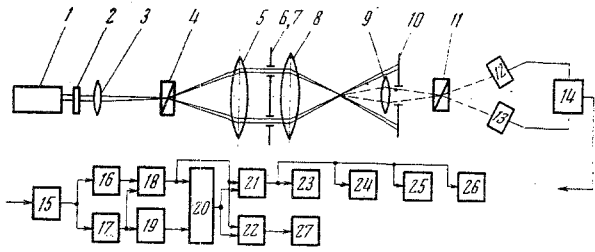


Fig. 1

Let us look at the measurement method. The attenuation of a laser beam when passed through the bubbly turbulent stream was used to determine the gas content in the experiment.

The relative attenuation of the laser beam under the indicated conditions can be represented in the form

$$\Delta I = f(l, \bar{C}, D_n),$$

where l is the path length of the beam in the two-phase medium, \bar{C} is the volumetric gas content of the medium, and D_n is the diameter of the bubbles which scatter the light.

To determine this dependence special studies were conducted on a calibration apparatus which consisted of a vessel with a porous bottom.

To exclude the first and third factors during the calibrations the path lengths of the laser beam in the two-phase medium of the test stream in the tube and in the calibration vessel were chosen as equal. In addition, to decrease the diameters of the bubbles generated by the permeable layer during the blowing of gas in the calibration vessel a 1% solution of ethyl alcohol was used instead of water. The mean bubble size was 150μ .

The volumetric gas content in the two-phase stream being studied was determined from the results of the calibration.

A Laser Doppler velocity meter (LDVM) developed at the Institute of Atomic Energy, Siberian Branch, Academy of Sciences of the USSR was used to study the average velocity field in single-phase and two-phase turbulent streams in a tube.

A diagram of the measurement apparatus is presented in Fig. 1. The optical part contains the sequential arrangement of a laser 1, a quarter-wave phase plate 2, an objective 3, a polarization splitter (a Wollaston prism) 4, an objective 5, diaphragms 6 and 7, a focusing objective 8, a receiver objective 9, a field diaphragm 10, a Wollaston prism 11, and photoreceivers 12 and 13 whose outputs are connected through a differential amplifier 14 to the electrical circuit for analyzing the Doppler signal. The Wollaston prism 4 is placed in the common focal plane of objectives 3 and 5 which form an afocal system.

The beam of the laser 1 after passing through the quarter-wave phase plate 2 is split by the polarization prism 4 into two orthogonally polarized beams having the same intensity. Since the objectives 3 and 5 form an afocal system, the split beams are parallel upon emergence from the objective 5. The opaque screen containing the diaphragms 6 and 7 serves to free the light beams from the noncoherent aureole. The split beams are focused by the objective 8 onto the test region of the stream.

In the region of intersection of the incident beams one can distinguish two orthogonal axes (x and y) which are turned by 45° angles relative to the orthogonal polarization vectors of the incident beams. The relative phase shift between the projections of the field vectors on the x axis and on the y axis will be characterized by π . The resultant light field can be represented as the superposition of two orthogonally polarized and spatially matched interference fields in which the bands are parallel and are out of phase while the envelopes are in phase.

The image of the probing field in the orthogonally polarized scattered beams is formed by the objective 9 and the prism 11 on the light-sensitive surfaces of the photoreceivers 12 and 13. The axes of the Wollaston prism 11 are turned by 45° relative to the polarization vectors of the incident beams. In this case the images of the interference fields with antiphase interference arrays in the scattered beams are separated and each is formed at its own photoreceiver. The light scattered from a particle passing through the probing region is modulated in intensity with a frequency inversely proportional to the period of the array.

One can show that the modulation frequency is equal to Doppler difference frequency [8]

$$f_D = U^2 \sin \alpha / \lambda, \quad (1)$$

where U is the measured projection of the velocity, 2α is the angle between the directions of the interfering beams, and λ is the wavelength of the laser radiation. The spatial-phase distribution of the intensity

in the probing interference field is transformed into the phase-time distribution by the moving scattering particle. Therefore, the output currents in each of the two photoreceivers are described by the respective equations

$$\begin{aligned} I_1 &= I_n(t) + I_D(t) \cos \omega t, \\ I_2 &= I_n(t) - I_D(t) \cos \omega t, \end{aligned} \quad (2)$$

where $\omega = 2\pi f_D$, I_n is the additive component of the signal, and I_D is the amplitude of the Doppler component.

The resultant current at the output of the differential amplifier 14 is determined as the difference between the output signals of the first and second photoreceivers [9].

Total suppression of the additive component of the signal and of the noise is not achieved in practice because of the depolarizing effect of the scattering particles.

Smooth regulation of the transmission coefficient is provided to make the output signals in each channel of the differential amplifier symmetrical. The subsequent processing of the Doppler signal is performed by the electronic assembly, which puts out the digital value of the velocity averaged over a given time and an analog voltage proportional to the instantaneous velocity. A simplified block diagram of the electronic part of the LDVM is shown in Fig. 1.

After preliminary amplification the signal enters an automatic filter unit 15 which automatically follows the maximum of the current spectrum of the Doppler signal. The filtered signal, which has the form of a random sequence of radio pulses symmetrical relative to zero, enters two threshold amplifier-limiters 16 and 17. From the output signals of these amplifiers the series of peaked counting pulses and the gate pulses whose duration corresponds to the duration of these series are formed by units 18, 19, and 20. The counting pulses and gate pulses enter a special counter 22 with a preassigned counting time. The counter gives digital readings directly in units of velocity. The counting time (averaged) can be varied in the range from 0.01 to 10 sec. The counter is provided with an output for sending the information to an electronic computer 27.

To obtain information on the "instantaneous" stream velocity the Doppler frequency is transformed into an analog signal by a frequency detector 21 with a memory, to which the same counting pulses and gate pulses are supplied. The fluctuations in the output voltage of the frequency detector are proportional to the deviations in the Doppler frequency and consequently to the velocity pulsations. The spectrum of the voltage pulsations corresponds to the spectrum of velocity pulsations. By feeding this voltage to instruments 23-26 one can determine the required statistical characteristics of the test stream, particularly the intensity and spectrum of the turbulence, the autocorrelation function of the pulses, etc.

The electronic assembly for processing the Doppler signal has three working subranges: 10-100 mm/sec, 100 mm/sec - 1 m/sec, and 1-10 m/sec. The corresponding bands of reproducible velocity pulsation frequencies are 0-10, 0-100, and 0-1000 Hz. The relative noise level at the analog output of the instrument does not exceed 0.01, which corresponds to a turbulent intensity of 1%.

An SK4-13 spectrum analyzer, which made it possible to evaluate the spectrum of the Doppler signal, was connected to the output of the differential amplifier in parallel with the electronic processing assembly. Since the Doppler spectrum is broadened because of modulation interference when the concentration of the gaseous phase is increased in the experimental region of the stream, the exact measurement of the mean Doppler frequency (the velocity) is difficult. In this case an approximate estimate (with an error of $\pm 5\%$) of the mean frequency of the spectrum at high concentrations was made from the spectrum analyzer.

The average and pulsation characteristics of the hydrodynamic friction at the bottom wall of the tube beyond the site of gas blowing were measured by a thermoanemometer of the RTPS type [10] with an end detector mounted flush with the wall. A platinum film with a size ($x \times z$) of $0.2 \times 2.5 \text{ mm}^2$, deposited by the brazing method on a substrate of hard glass, served as the detector. The signal from the detector according to [11] is proportional to the average velocity gradient at the wall, i.e., to the shear stress of the viscous friction.

The pulsation component of the signal from the detector went to the input of a spectral analyzer of type 2112 of the Bruhl and Kier Company with three-octave band-pass filters and was recorded on a 2305 type recorder.

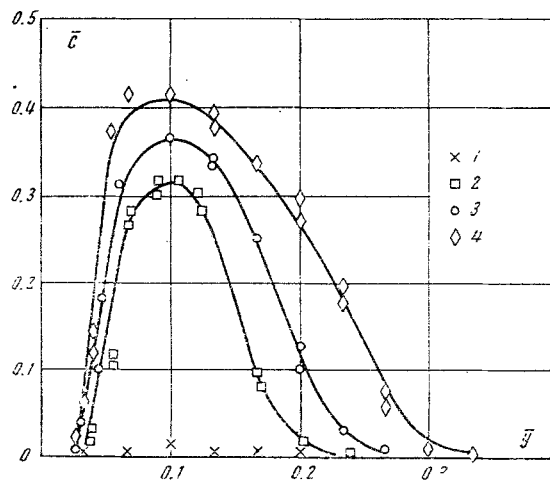


Fig. 2

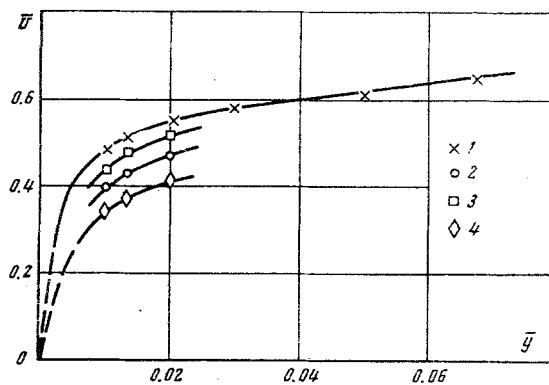


Fig. 3

The different characteristics of the two-phase stream were measured in a cross section of the working part of the tube located 50 mm beyond the permeable layer. All the measurements were conducted at a stream velocity of $U_m = 8.3$ m/sec at the axis of the tube. The Reynolds number, determined from the hydraulic diameter of the tube, was $\sim 2.2 \cdot 10^5$.

The distribution of the volumetric gas content over the cross section of the working part of the tube for different modes of gas saturation of the stream is shown in Fig. 2.

The dimensionless distance from the bottom wall of the tube $\bar{y} = 2y/H$, where $H = 30$ mm is the height of the working section of the tube, is laid out along the abscissa, while the volumetric gas content \bar{C} is laid out along the ordinate. Here $C_q = Q/U_m S_1$ is the dimensionless coefficient of the gas flow rate, Q is the volumetric gas flow rate, and S_1 is wetted area of the permeable layer. The values of C_q for points 1-4 are $(0.29, 1.72, 2.60, 4.3) \cdot 10^{-3}$, respectively.

We can note three of the principal features of the distribution of the volumetric gas content in a turbulent stream beyond the site of gas blowing: first, in the immediate vicinity of the bottom wall of the tube (in the viscous sublayer) the volumetric gas concentration is equal to zero; second, the maximum of the volumetric gas content occurs at $\bar{y} \approx 0.1$; third, as one moves toward the axis of the tube the volumetric gas content decreases smoothly to zero.

The reason for the existence of a zone of pure liquid in the immediate vicinity of the bottom wall and for the concentration of small gas bubbles at some distance from it evidently is the Zhukovskii force, connected with the considerable circulation of the velocity around the gas bubbles which have just separated from the permeable layer, and the buoyant force of the bubbles.

The average velocity profiles for the modes of gas saturation corresponding to Fig. 2 are shown in Fig. 3.

The average velocity profile in a single-phase stream is shown in Fig. 3 by a solid line. It corresponds well to a $1/7$ power law for a turbulent stream in a tube. The velocity profile in the two-phase

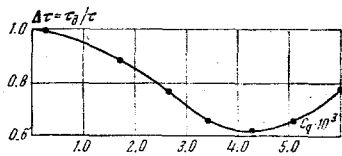


Fig. 4

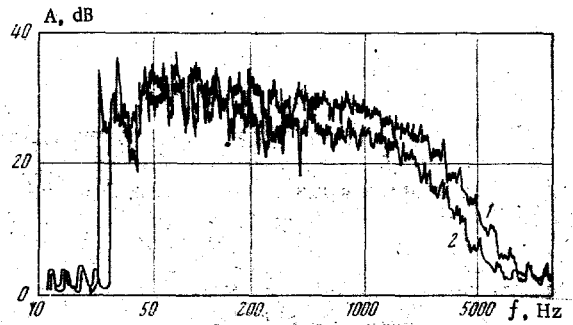


Fig. 5

with the film end detector, is shown in Fig. 4. It follows from the graph that the larger the volumetric gas content of the stream, the smaller the shear stress at the bottom wall of the tube. The presence of an optimum gas flow rate at which the reduction in friction is maximal is characteristic.

The results of the thermoanemometric measurement can be compared with the data on the measurement of the velocity profile in Fig. 3. On the assumption that the liquid in the viscous sublayer is Newtonian ($\bar{C} = 0$) the estimates of the reduction in local friction based on the data of Figs. 3 and 4 coincide with the accuracy of the measurement error.

The rms spectra of the pulsations in friction in a single-phase stream (1) and at the optimum gas saturation (2) are shown in Fig. 5.

The pulsation frequencies (Hz) are laid out along the abscissa and the rms value of the friction pulsations A in a logarithmic scale along the ordinate. The greatest change in the intensity of friction pulsations with gas saturation of a turbulent stream in a tube occurs in the region of frequencies from 200 to 4000 Hz and comprises 5 dB at the optimum gas content of the stream, i.e., the intensity of the friction pulsations is decreased by almost 1.5 times. This indicates the distinctive stabilization of the flow in the boundary zone caused by small gas bubbles at high volumetric gas contents.

The results of the experimental studies indicate that a considerable reduction in the local hydrodynamic resistance takes place upon the gas saturation of a turbulent stream in a tube. With the reduction in the hydrodynamic resistance the average velocity gradient at the wall over which the flow occurs is reduced by the same value. The spectral characteristics of the pulsations in hydrodynamic friction show that the reduction in friction produced by small gas bubbles at high volumetric concentrations is connected with stabilization of the flow in the boundary zone. The distribution of the volumetric gas concentration in the turbulent stream is distinctive: its maximum occurs at $\bar{y} = 0.1$, while in the immediate vicinity of the wall over which the flow occurs (in the viscous sublayer) gas bubbles are absent.

LITERATURE CITED

1. L. G. Loitsyanskii, "On changing the resistance of bodies by filling the boundary layer with liquids having other physical constants," *Prikl. Matem. i Mekhan.*, **6**, No. 1 (1942).
2. K. K. Fedyavskii, "Decrease in frictional resistance through a change in the physical constants of the liquid at the wall," *Izv. Akad. Nauk SSSR, Otd. Tekh. Nauk*, Nos. 9-10, (1943).
3. V. N. Isachenkov, "Viscosity of a gas-saturated liquid," in: *Proceedings of the Institute of Hydrodynamics, Siberian Branch, Academy of Sciences of the USSR* [in Russian], Novosibirsk (1963), pp. 16-23.
4. H. Shigeru and O. Morimatsu, "The relationship between the apparent viscosity and the void fraction in two-phase flow," *Bull. Japan. Soc. Mech. Eng.*, **14**, No. 75 (1971).
5. A. M. Basin, A. I. Korotkin, and L. F. Kozlov, *Control of the Boundary Layer of a Ship* [in Russian], Sudostroenie, Leningrad (1968).

stream was not measured completely since at volumetric concentrations greater than 3% the laser beam was so attenuated that the Doppler signal could not be distinguished from the noise.

It is seen from the graph that the larger the volumetric gas content in the turbulent stream, the smaller the average velocity gradient at the bottom wall of the tube.

It must be taken into account that because of the large velocity gradient in the zone near the bottom wall the largest critical dimension of the region of spatial resolution of the LDVM was the component along the y axis, which in the experiment equalled 30μ . The entire region of spatial resolution comprised a volume $x \times y \times z$ of $(0.03 \times 0.6 \times 3 \text{ mm}^3)$, respectively.

The dependence of the relative hydrodynamic resistance $\Delta\tau = \tau_0/\tau$ on the gas flow rate, obtained from the results of the thermoanemometric measurements

6. L. Tong, *Boiling Heat Transfer and Two-Phase Flow*, Wiley (1965).
7. S. S. Kutateladze and A. M. Styrikovich, *Hydraulics of Gas-Liquid Systems* [in Russian], Gosénergoizdat, Moscow-Leningrad (1958).
8. G. A. Barill, Yu. G. Vasilenko, Yu. N. Dubnishchev, and V. P. Koronkevich, "Fourier analysis of laser Doppler devices," *Avtometriya*, No. 5, 41-47 (1973).
9. Yu. G. Vasilenko, Yu. N. Dubnishchev, and E. N. Utkin, "On reducing the level of additive interference in the output signal of a laser velocity meter," *Opt. i Spekr.*, 35, No. 2, 366-369 (1973).
10. A. A. Stolpovskii, N. I. Tkachev, and E. N. Utkin, "Self-compensating devices for measuring the parameters of streams of liquids and gases," in: *Devices and Elements of Systems for the Automation of Scientific Experiments* [in Russian], Nauka, Novosibirsk (1970).
11. B. J. Bellhouse and D. L. Schultz, "Determination of mean and dynamic skin friction, separation and transition in low-speed flow with a thin-film heated element," *J. Fluid Mechan.*, 24, Part 2 (1966).